JAERI-M
4438

Kinetics of Carbon Transfer between Uranium Carbide Fuel and Stainless Steel bonded with Sodium

May 1971

G. Nishio・J. Shimokawa

日本原子力研究所
Japan Atomic Energy Research Institute

JAERI－M　4438

ナトリウムでボンドされた炭化ウラン燃料とステンレス鋼間の炭素移行現象に関する研究

日本原子力研究所東海研究所燃料工学部
西尾軍治・下川純一

（１９７１年５月受理）

〔要旨〕　この研究は，炭化物燃料とステンレス鋼の両立性を支配する炭素移行現象の機構をあきらかにするため行なったものである。Naが充填されたNiカプセル内に ^{14}CでラベルしたUC 燃料とステンレス鋼（AISI　304）を挿入，その系を７５０℃で加熱，適当な時間間隔で出された鋼中の放射能を測定，鋼内に浸炭した ^{14}Cの濃度分布を求めた。

浸炭現象に起因した濃度分布式は，炭化物燃料から鋼への炭素の移行が『燃料内UC_2中の炭素がNa によって浸出される』という，いわゆる脱炭機構とステンレス鋼の浸炭が『炭素原子の粒界拡散に基づく』という拡散機構を結合したモデルから求められた。

実験から得られた鋼中の ^{14}C の分布値は，このモデルより計算した値と比較的良く一致し，この結果から，燃料の脱炭速度が鋼の浸炭の度合を律していること，また鋼の浸炭相は，粒界にそって生長してゆくことがあきらかになった。

JAERI - M 4438

Kinetics of Carbon Transfer between Uranium Carbide Fuel and Stainless Steel bonded with sodium.

Gunji Nishio and Junichi Shimokawa

Division of Nuclear Fuel Research, Tokai, JAERI

(Received April 1971)

Abstract The purpose of the present study was to provide information on the kinetics of carbon transfer governing the degree of compatibility between carbide fuel and austenitic stainless steel, by comparing the experimental with the calculational results.

Hyperstoichiometric uranium carbide containing ^{14}C (6.0 wt.% carbon) and stainless steel (AISI 304) specimen were enclosed in a nickel capsule together with sodium, and then this capsule was heated at 750°C according to the predetermined schedule. The degree of carburization of the steel was determined by counting ^{14}C with a 2α gas-flow counter. The distribution profile of ^{14}C seemed to be nearly exponential and the radioactivity on the sectioning surface of the stainless steel specimen increased with increase of the heating time.

The kinetics of carbon transfer was well interpreted by assuming that carbon atoms were leached out into sodium from UC_2 platelets; in which they had precipitated in the UC and then diffused along the grain boundaries of stainless steel accompanied by the formation of new carbide such as $Cr_{23}C_6$.

目　次　な　し

1. Introduction

Uranium-plutonium mixed carbides are considered as promising nuclear fuel for high-gain fast reactor. The utilization depends on the availabilities of stable carbides for sodium, and of cladding materials compatible with the fuels.

Stoichiometric and hypostoichiometric carbides are not decarburized below the boiling point of sodium[1,2], but preperation of the precisely stoichiometric uranium carbide is much difficult. On the other hand, the hypostoichiometric uranium carbide containing free uranium metal is not suitable, because of relatively large swelling and low melting point of the free metal, and of eutectic reaction between the free metal and cladding material.

Many experiments have been carried out on compatibility between higher carbide fuel and austenitic stainless-steel claddings bonded with sodium. It is metallographically revealed that the decarburization of the fuel and the carburization of the steel are respectively governed by disolution of carbon atoms from the fuel and by diffusion of carbon atoms in the steel. The lifetime of stainless steel cladding on the compatibility may be restricted by degree of the brittleness due to carbon transfer from the carbide fuel to its cladding. However, theoretical studies on the compatibility are relatively little[3], because of complex behavior of carbon atoms in fuel and cladding material.

Purpose of the present study was to provide information on the kinetics of carbon transfer governing the degree of compatibility between carbide fuel and austenitic stainless steel. Hyperstoichiometric uranium carbide containing ^{14}C was used for obtaining the distribution profile of carbon atoms in the austenitic stainless steel (AISI 304). The mechanism was investigated from the viewpoint of the disolution of carbon atoms from UC_2 platelets precipitating in UC matrix, and the migration of carbon atoms along the diffusivity path in which a grain boundary of the stainless steel is included. The carbon distribution profiles could be almost interpreted by Fisher's theory on the grain boundary diffusion[4].

2. Experimental procedure

The austenitic stainless steel (AISI 304) was preliminarily annealed at 1100°C for 15 minutes and then quenched. Carbide specimens were made by arc melting mixture of uranium metal and graphite labeled with ^{14}C (specific activity $\gamma = 8.2 \times 10^7$ cpm/g-carbon). The uranium carbide

containing 6.0 wt.% carbon included some amounts of UC_2 platelets (Widmanstätten) precipitated in the UC matrix. Carbide and stainless steel specimens were machined so that their surface areas effective to carbon transfer became about $S_c = 0.96$ and $S_s = 4.0$ cm^2, respectively.

Both the specimens were enclosed in a nickel capsule together with reactor grade sodium and a Zr-Ti foil as shown in Fig. 1. Then the capsule was sealed up by fusing under the helium gas atmosphere. For elimination of oxygen in sodium by Zr-Ti foil, first this capsule was heated at 600°C for 15 days in an upright position so that the sodium covered the foil. Next, the capsule was turned upside down and then heated at 750°C for predetermined period of time. After heating, only a stainless steel specimen was ground parallel to the original surface. Thickness of the layer cut off was determined by measuring the difference in weight of the specimen before and after sectioning.

The distribution profile of carbon atoms was determined by counting ^{14}C on the ground surface of the specimen with a 2π type gas-flow counter. The relation of the depth of sectioning and the counting on the sectioning surface was obtained as shown in Fig. 2; this relation seemed to be nearly exponential in all expriments. The radioactivity on the sectioning surface increased with the increase of heating time.

3. Decarburization phenomenon in carbide

It is well known that depletion of carbon atoms from the hyperstoichiometric uranium carbide (mainly from UC_2 platelets precipitating in UC matrix) occurs by the reaction $UC_2 \xrightarrow{Na} UC + C$ (leached out in sodium), and therefore the frontal edge of the decarburized zone of UC_2 platelets, namely, the sodium - UC_2 interface advances toward the interior from the fuel surface as decarburization proceeds. The reaction at the interface leaves UC phase and a void at a UC_2 platelets site. As the interface proceeds, these void are interconnected where UC_2 platelets had previously formed a continuous network. The sodium permeates the void, therefore a channel filled up with sodium is made along the previous network of UC_2 platelets. The UC phase formed by the reaction may not longer react with sodium, if highly purified sodium is used.

Decarburization studies by Elkins[1], by Webb[2], and by Watanabe et.al.[5] show that the depth, $(\bar{X})$, of the decarburized layer in the carbide specimen is proportional to the exposure time as shown in Fig. 3, and that the decarburization rate is independent of the original carbon content

of the carbide, but it increases with temperature of sodium. The decarburization rate (cm/sec), i.e. the slop of lines in Fig. 3, are plotted against the reciprocal absolute temperature as shown in Fig. 4. From the straight line obtained by the curve fitting method, the decarburization rate can be expressed as

$$\frac{dX}{dt} = 0.0035 \exp(-26{,}800/RT). \quad \cdots\cdots \quad (1)$$

The activation energy is 26.8 kcal/mole, which is fairly small in comparison with the value of 60 ~ 80 kcal/mole for the activation energy of the diffusion of carbon atoms in the uranium carbide[6].

Consequently the decarburization process of higher carbide containing UC_2 can be interpreted by "the disolution of carbon atoms in UC_2" rather than by diffusion of carbon atoms through UC to the fuel surface, because of the independence between the decarburization rate and carbon content.

4. Analytical treatments

4.1 Decarburization and carbon transfer in carbide

Degree of carburization of the stainless steel is considered to be governed by the decarburization rate of carbide fuel. Therefore, calculation of flux of the excess carbon atoms from the carbide becomes much important.

Well, volume fraction of the voids formed from UC_2 platelets as shown in Fig. 5, that is, volume fraction of whole channels made in the decarburized layer of the carbide specimen is given by

$$\triangle V/(V_{UC} + V_{UC_2}) = (V_{UC_2} - V'_{UC}) / (V_{UC} + V_{UC_2}) \quad \cdots\cdots \quad (2)$$

where

$$V_{UC} = A\,(M/\rho)_{UC}$$

$$V_{UC_2} = B\,(M'/\rho')_{UC_2} \quad \cdots\cdots\cdots\cdots \quad (3)$$

and

$$V'_{UC} = B\,(M/\rho)_{UC}\,.$$

On the other hand, the weight percentage of carbon atoms in the original carbide is

$$W\ (\text{wt. \%}) = (4.80A + 9.16B) / (A + B). \quad \cdots\cdots\cdots (4)$$

Here, $\triangle V$ is the volume of the voids formed from UC_2 platelets; V_{UC} and V_{UC_2} are the volumes of UC matrix and of UC_2 platelets; and V'_{UC} is the volume of UC newly formed in the channels of UC_2 platelets. A and B are also the molarities (mole) of UC and of UC_2; and $(M/\rho)_{UC}$ and $(M'/\rho')_{UC_2}$ the molecular volumes (cm^3/mole) of UC and of UC_2 phase.

Substituting Eqs. (3) and (4) to Eq. (2) leads to

$$\triangle V/V = \frac{(\frac{9.16-W}{4.36})(\frac{M}{\rho})_{UC} + (\frac{W-4.80}{4.36})(\frac{M'}{\rho'})_{UC_2} - (\frac{M}{\rho})_{UC}}{(\frac{9.16-W}{4.36})(\frac{M}{\rho})_{UC} + (\frac{W-4.80}{4.36})(\frac{M'}{\rho'})_{UC_2}} \quad \cdots\cdots (5)$$

Assuming that the carbon atoms leached out from the decarburized layer of the carbide move to the stainless steel through sodium phase without loss, and that inner wall of the used nickel capsule is not carburized, the arrival rate of the carbon atoms onto unit area of the stainless steel, this is, the flux of carbon atoms is given by

$$J = 2.25\ (dX/dt)(\triangle V/V)(S_c/S_s). \quad \cdots\cdots\cdots\cdots (6)$$

Here, 2.25 (g/cm^3) is the density of graphite, and S_c and S_s are the surface areas of carbide and stainless steel specimens, respectively.

4.2 Carburization and carbon transfer in stainless steel

The carburization of austenitic stainless steel is considered to be governed by grain boundary diffusion[7] as shown in Fig. 6. Therefore the following equations can be applied to analyzing the carbon transfer in the stainless steel.

$$\frac{\partial C}{\partial t} = D_b \left(\frac{\partial^2 C}{\partial X^2}\right) + \frac{2 D_v}{\delta}\left(\frac{\partial C}{\partial y}\right)_{y=0} \qquad \cdots\cdots\cdots (7)$$

$$\frac{\partial C}{\partial t} = D_v \left(\frac{\partial^2 C}{\partial y^2}\right)$$

where X axis is taken normal to the original surface of the steel, y axis normal to the grain boundary, t the time, C the concentration (g-carbon/cm^3) of carbon atoms at any position within the steel, and δ the width of carbon-diffusivity path (so called grain boundary slab) in which a grain boundary is included. D_v is the apparent volume-diffusion coefficient, and D_b the apparent grain-boundary diffusion coefficient.

If semi-infinite model is applicable, the boundary conditions are:

$$\begin{aligned} C(X, 0, t) &= \phi(X) \\ C(X, \infty, t) &= 0 \\ C(\infty, y, t) &= 0 \\ J &= -D_b (dC/dX)_{X=0} + 2 D_v (dC/dy)_{y=0} \end{aligned} \qquad \cdots\cdots\cdots (8)$$

Here, $\phi(X)$ gives the concentration (g/cm^3) of carbon atoms only in the grain boundary slab (refer to Fisher's analysis)[4], and J the flux of carbon atoms transferred from the carbide to the surface of stainless steel. Using above the boundary conditions, the solution of Eq. (7) is approximately given as

$$C(X, y, t) = \frac{J \exp\{-\xi(t) X\}}{D_b \xi(t) - 2\sqrt{D_v/\pi t}} \operatorname{erfc} \frac{y}{\sqrt{4 D_v t}} \qquad \cdots (9)$$

where

$$\xi(t) = \frac{\sqrt{2}}{(\pi D_v t)^{1/4}} \sqrt{\frac{D_v}{D_b}}$$

The radio-assaying observation is expressed by means of a diffusion penetration curve, which gives the quantity (cpm/cm^2) of diffusing carbon atoms that has reached any sectioning surface. Therefore, the theoretical penetration curve is obtained by integration Eq. (9) over y

and using the specific activity r (cpm/g-carbon).

$$C_s(X, t) = \int_{-\infty}^{\infty} C(X, y, t)\, dy$$

$$= \frac{4J}{r}\sqrt{\frac{D_v t}{\pi}}\ \frac{J \exp\{-\xi(t) X\}}{D_b \xi(t) - 2\sqrt{D_v/\pi t}} \qquad \cdots\cdots\cdots (10)$$

5. Discussion

The diffusing carbon atoms reacts naturally with some elements such as chromium in stainless steel to follow the formation of new carbide such as $Cr_{23}C_6$. Therefore, it is considered that diffusing carbon atoms tend to sink around the sites of their acceptors. However, since no consideration on sink effect is taken in diffusion equations such as Eq. (7), only apparent diffusion coefficients are obtained as already done in the previous work[7].

Diffusivity paths including grain boundaries of stainless steel were clearly observed microscopically; width of a path was measured to be 2 ~ 4μm thick.

- Mathematical calculation -

Data used for mathematical calculation by Eq. (10) are as follows:

Carbon weight percentage of the original carbide: $W = 6.0$ wt.%

Surface area of the carbide: $S_c = 0.96$ cm^2

Surface area of the stainless steel: $S_c = 4.0$ cm^2

Specific activity of ^{14}C: $r = 8.2 \times 10^7$ cpm/g-carbon

Molecular weights of UC and UC_2: $M_{UC} = 250$, $M'_{UC_2} = 262$ g/mol

Densities of UC and UC_2: $\rho_{UC} = 13.08$, $\rho'_{UC_2} = 11.68$ g/cm^3

Apparent volume diffusion coefficient: $D_v = 6.2 \times 10^{-13}$ cm^2/sec

Apparent grain boundary diffusion coefficient:

$D_b = 0.9 \times 10^{-9}$ cm^2/sec

Width of diffusivity path: $\delta = 3\mu$m

Heating temperature: $T = 750$°C

Since $\triangle V/V = 0.058$ and $dX/dt = 10^{-8}$ cm/sec, the flux of carbon atoms was calculated to be 3.1×10^{-10} (g-carbon/cm^{2}sec) from Eq. (6). Fig. 7 gives the profiles of ^{14}C activity in the stainless steel. The theoretical penetration curves obtained from Eq. (10) are also shown in this figure.

From these results it may be considered that (1) if hyperstoichiometric carbide is used as donar of carbon atoms, the magnitude of carbon flux onto stainless steel is governed by decarburization rate of the carbide, and (2) kinetics of carburization of stainless steel is interpreted with a relatively good tendency from the grain boundary diffusion mechanism.

Symboles

A	Molarity of UC (mole)
B	Molarity of UC_2 (mole)
C	Concentration of carbon at any position within stainless steel (g/cm^3)
C_s	Activity of ^{14}C per unit area of sectioning surface (cpm/cm^2)
D_b	Apparent grain-boundary diffusion coefficient (cm^2/sec)
D_v	Apparent volume diffusion coefficient (cm^2/sec)
J	Flux of carbon atoms transferred from carbide to stainless steel (g/cm^{2}sec)
M_{UC}	Molecular weight of UC (g/mol)
M'_{UC_2}	Molecular weight of UC_2(g/mol)
R	Gas constant
S_c	Surface area of carbide specimen (cm^2)
S_s	Surface area of stainless steel (cm^2)
T	Absolute temperature of sodium bonding (°K)
t	Time of heating (sec)
V_{UC}	Volume of UC matrix (cm^3)
V'_{UC}	Volume of UC formed from UC_2 platelets within carbide (cm^3)
V_{UC_2}	Volume of UC_2 platelets (cm^3)
$\triangle V$	Volume of void formed from UC_2 platelets (cm^3)
V	Volume of carbide fuel (cm^3)
W	Weight percentage of carbon in the original carbide fuel (%)
X	Distance from the original surface of stainless steel (cm)
y	Distance normal to the grain boundary slab (cm)
γ	Specific activity of ^{14}C (cpm/g-carbon)
δ	Thickness of the diffusivity path (cm)

ρ_{UC} Density of UC (g/cm^3)
ρ'_{UC_2} Density of UC_2 (g/cm^3)

References

(1) P.E. Elkins "Compatibility of uranium carbide fuels with cladding materials", NAA-SR-7502 (1964)

(2) B.A. Webb "Carburization of austenitic stainless steel by uranium carbide in sodium systems", NAA-SR-6246(1963)

(3) V.S. Eremeev, et.al. "Diffusion of carbon from uranium carbide into molybdenum and tungsten" LA-TR-67-31 (1967) Thermodyn. Proc. Symp., Vienna, 1965, 2, 161 (1966)

(4) J.C. Fisher "Calculation of diffusion penetration curves for surface and grain boundary diffusion" J. Appl. Phys. 22, 74 (1951)

(5) H. Watanabe, et.al. "Reaction between uranium carbide and liquid sodium", JAERI-memo 4347 (1971)

(6) T.C. Wallace, et.al. "Carbon diffusion in the carbides of uranium", LA-DC-8840 (1968)

(7) G. Nishio, J. Shimokawa "Process of carburization in austenite stainless steel", JAERI-memo 4132 (1970)

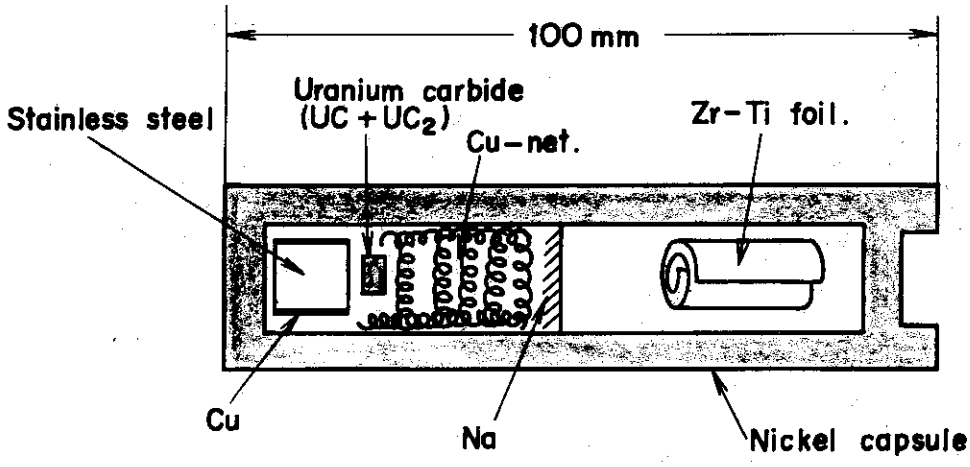

Carbon Weight Percentage of Uranium Carbide ------ 6.0 Wt. %

Austenitic Stainless Steel ---------- AISI 304

Specific Activity of ^{14}C in the carbide --------- 8.2×10^7 cpm/g-carbon

Temperature of Annealing ---------- 750°C

Surface areas ---------- $S_c = 0.96\ cm^2$, $S_s = 4.0\ cm^2$

Fig. 1 Nickel capsule consisting of uranium carbide containing UC_2 phase, and austenite stainless steel bonded with sodium ; Zr-Ti foil is enclosed as oxygen-trapping material.

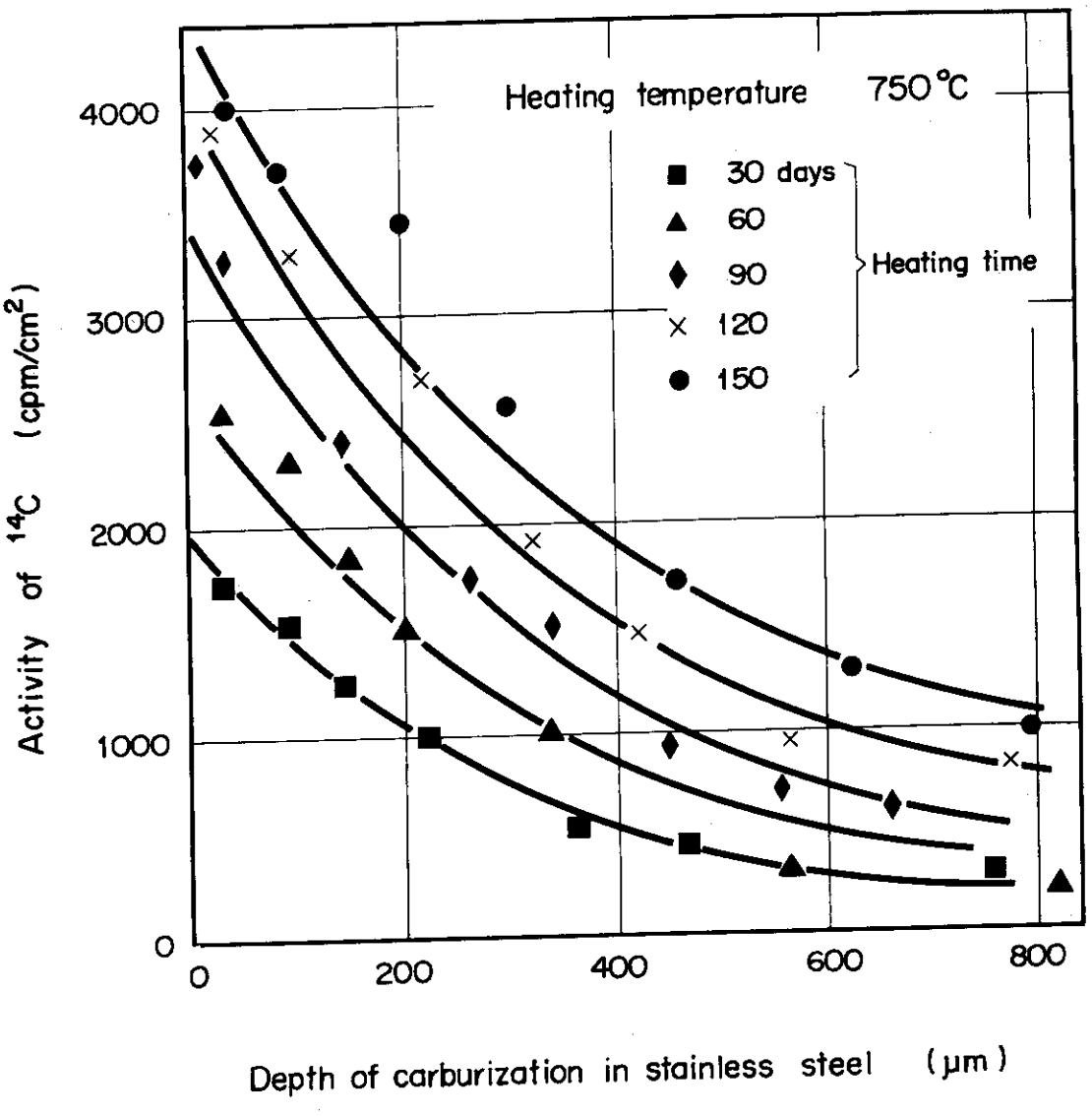

Fig. 2 Distribution profiles of ^{14}C in stainless steel exposed to sodium at 750 °C

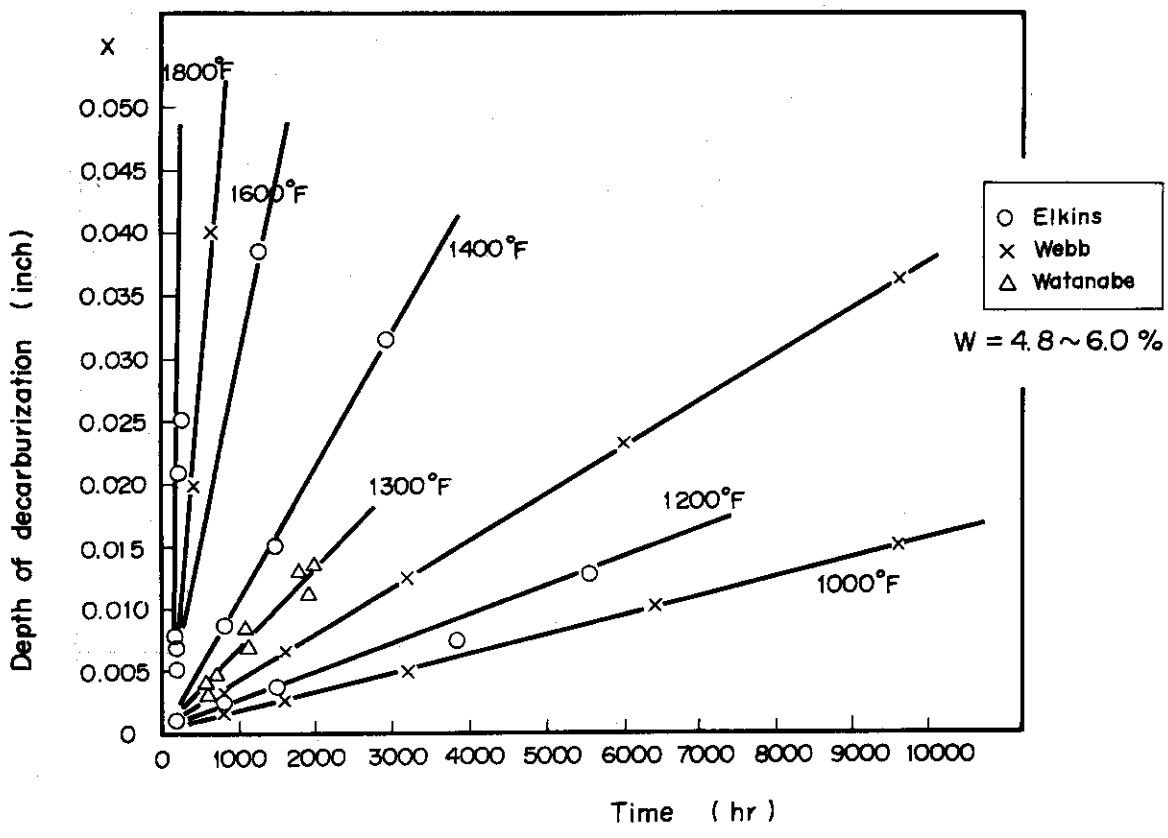

Fig. 3 The variation of the decarburization depth (inch) of hyperstoichiometric uranium carbide containing UC_2 with the exposure time (hrs) in sodium, in the temperature range of 1000 to 1800°F

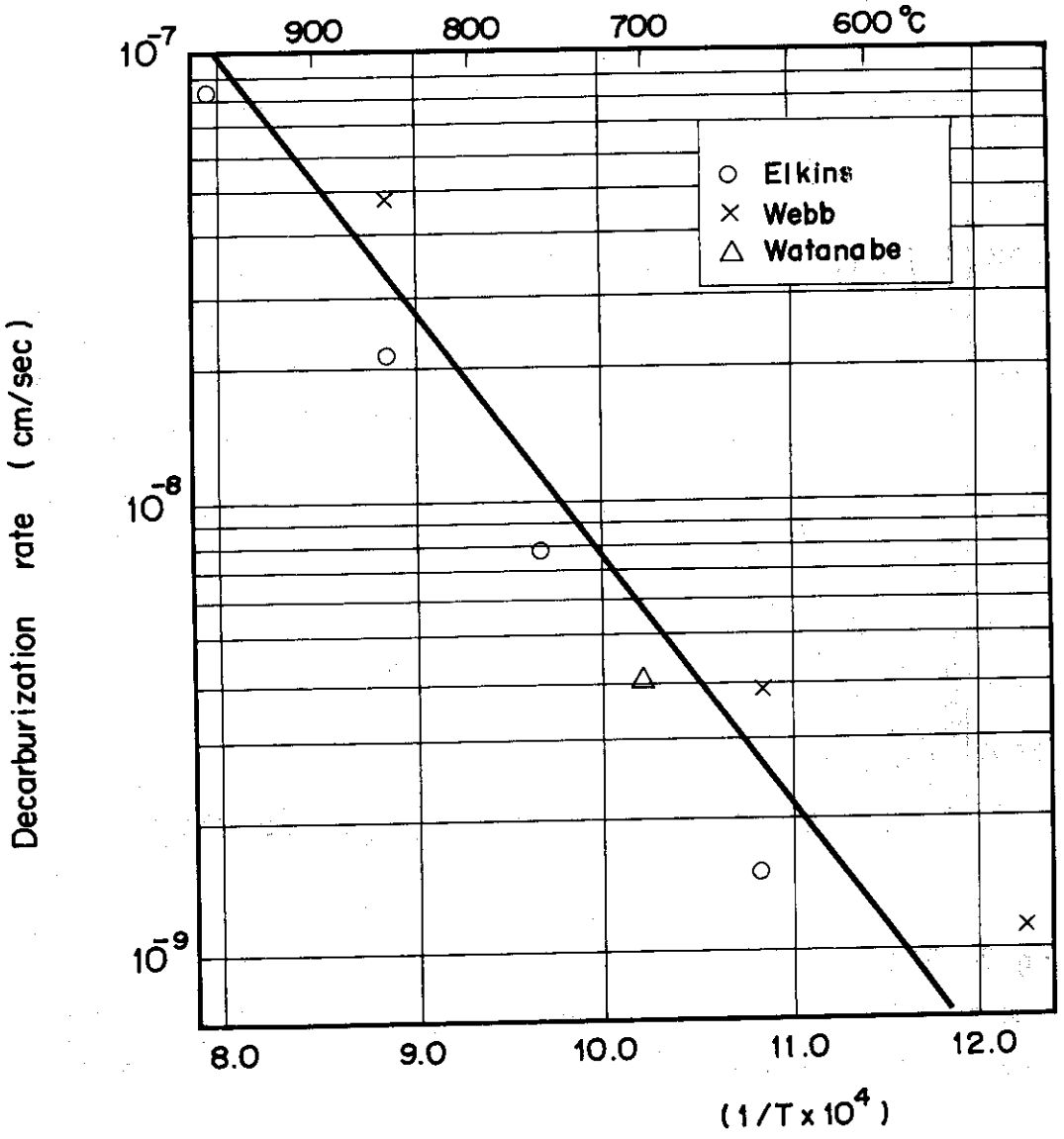

Fig. 4 The dependece of temperature on the decarburization rate of the hyperstoichiometric uranium carbide containing UC_2; activation energy is 26.8 kcal/mole.

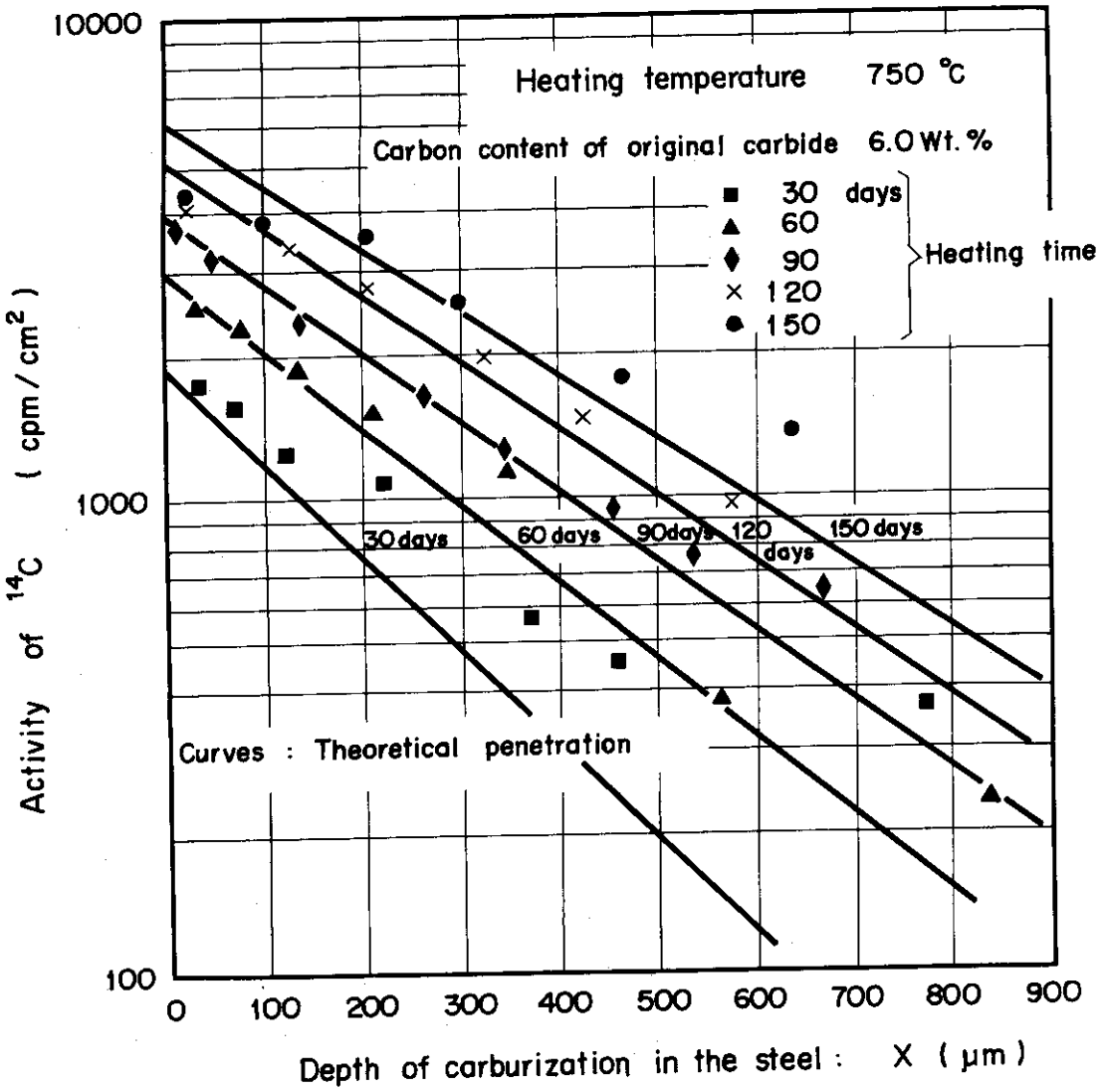

Fig. 7 Experimental data on ^{14}C activity in stainless steel and theoretical penetration curves.

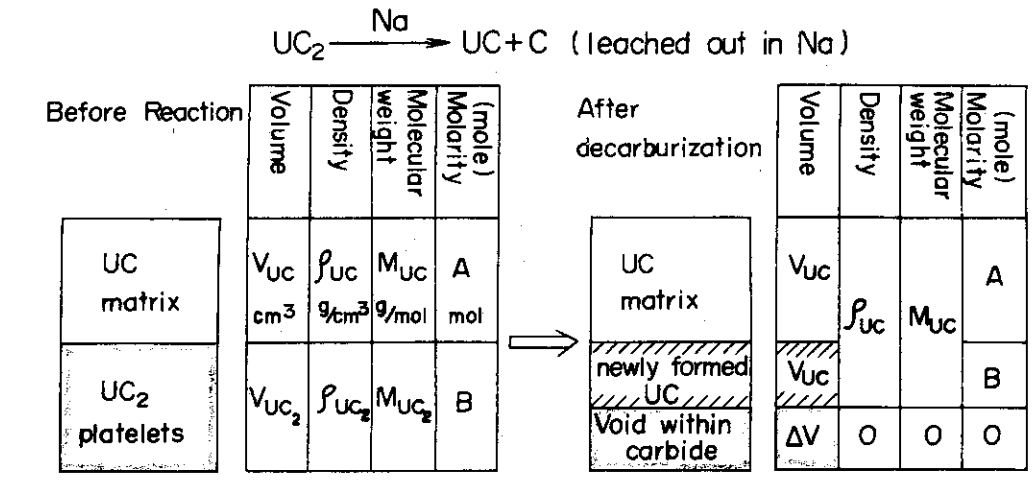

Fig. 5 Composition change of carbide fuel specimen after decarburization

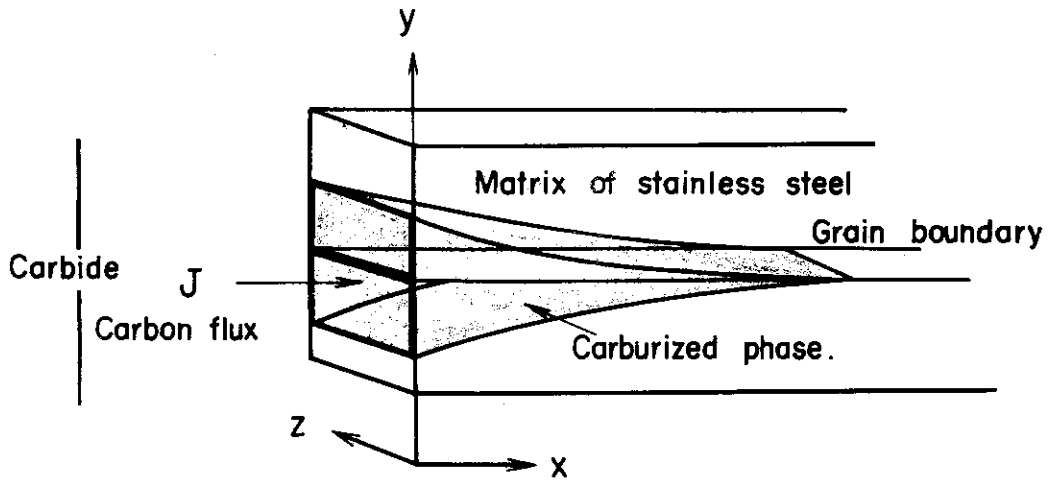

Fig. 6 Scheme of ^{14}C distribution in stainless steel by grain-boundary diffusion; the carburized path is shown by shadowgraph along the grain boundary.